28 Apr 1981, 9:00 am - 12:30 pm

Assessment of Liquefaction Potential Based on Seismic Energy Dissipation

R. O. Davis
University of Canterbury, New Zealand

J. B. Berrill
University of Canterbury, New Zealand

Proceedings: First International Conference on Recent Advances in Geotechnical Earthquake Engineering and Soil Dynamics, April 26 - May 3, 1981, St. Louis, Missouri

Assessment of Liquefaction Potential Based on Seismic Energy Dissipation

R. O. Davis and J. B. Berrill

Department of Civil Engineering, University of Canterbury, Christchurch, New Zealand

SYNOPSIS: A simple relationship between dynamic pore pressure increase, earthquake magnitude, epicentral distance, initial effective overburden stress, and SPT value is proposed. The model is based on the concept that pore pressure increase depends upon the density of seismic energy dissipated at the site.

INTRODUCTION

Conventional analyses of liquefaction potential involve the basic concept that the dynamic pore pressure increase depends upon the magnitude of deviatoric stress and the number of stress reversals which may occur at a given site. The parameters stress magnitude and number of cycles are particularly convenient for use in interpretation of laboratory results, but are somewhat nebulous when used in interpreting actual field behaviour of soils under highly irregular seismic loading conditions. As a result, the concepts of equivalent uniform stress level and equivalent number of cycles (Seed and Idriss, 1970) have been introduced and widely used. In contrast to the stress based approach, Nemat-Nasser and Shokooh (1979) have suggested that dynamic pore pressure increase depends upon the density of dissipated energy during cyclic loading. They have compared their analysis with laboratory test data and shown that the proposed relationship closely matches test results. Although they did not consider actual seismic loading in true field situations, it seems clear that dissipated energy may be a more convenient parameter than equivalent stresses and equivalent numbers of cycles for characterization of actual earthquake loading.

In this article, we combine the concept of Nemat-Nasser and Shokooh (1979) with simple relationships between earthquake magnitude, radiated seismic energy, and energy dissipation to obtain an expression for dynamic pore pressure buildup. The total radiated seismic energy is obtained from the earthquake magnitude by the relationship of Gutenberg and Richter (1956). A simple geometric attenuation argument then leads to the arriving seismic energy density at the potentially liquefiable site. We characterize the site dissipation properties by the initial effective overburden stress and the corrected SPT value. Dependence of energy dissipation on the site SPT value is determined by a statistical analysis of 59 liquefaction case histories. Our main result, equation (11), gives the expected pore pressure increase as a function of two earthquake parameters: magnitude and epicentral distance, and two site parameters: initial effective overburden stress and SPT value.

SITE ENERGY DENSITY

We consider level ground, initially free from shear on horizontal planes, composed of saturated sand. Should an earthquake occur nearby, seismic waves propagating from the rupture carry energy to the site. The density of arriving energy depends upon the total radiated energy as well as whatever attenuation occurs between source and site. The total radiated energy E is related to earthquake magnitude through the well known expression of Gutenberg and Richter (1956)

$$E = a\,10^{-1.5M} \tag{1}$$

where M is magnitude and a is a constant with dimensions of energy. If SI units are employed, a is given by

$$a = 10^{1.8}\ \text{kJ} = 63.1\ \text{kJ} \tag{2}$$

The fraction of E which actually arrives at the site may depend upon many factors. Radiation pattern and directivity effects may focus the radiated energy more in one direction than another. Both geometric and material attenuation will also alter the arriving energy density. It should be noted that all of these factors also effect the stress time history at the site. Because the exact radiation pattern is impossible to predict in advance, we shall assume isotropic energy radiation. In order to further simplify our result, we also ignore material attenuation effects, and employ the following simple geometric attenuation model. Consider a hemispherical shell with unit thickness centered at the earthquake epicentre. The radius of the shell is r, the epicentral distance. In the absence of material attenuation, the entire radiated energy E must pass through this shell, and, assuming isotropic radiation, the energy density within the shell will be independent of position. Then the energy density, ε, arriving at the site is a function only of r and M, given by

$$\varepsilon(r,M) = E/2\pi r^2 = a\,10^{1.5M}/2\pi r^2 \tag{3}$$

ENERGY DISSIPATION AND PORE PRESSURE INCREASE

We denote the dissipated energy density at the site by $\Delta\varepsilon$, and we assume the following relationship between $\Delta\varepsilon$ and the arriving energy density ε

$$\Delta\varepsilon = \Gamma(\bar{\sigma}_o,\bar{N})\,\varepsilon(r,M) \tag{4}$$

Here $\Gamma = \Gamma(\bar{\sigma}_o,\bar{N})$ is the site dissipation function which depends upon the initial site overburden stress, $\bar{\sigma}_o$, and the corrected site SPT value, $\bar{N}$. Both $\bar{\sigma}_o$ and $\bar{N}$ refer to the average values within the potentially liquefiable soil deposit. We use the SPT correction of Peck, Hanson, and Thornburn (1974)

$$\bar{N} = 0.77 \log(2000/\bar{\sigma}_o)N \tag{5}$$

where N is the raw SPT value, $\bar{\sigma}_o$ has dimensions of kPa, and the logarithm has the base 10. Equation (5) biases the SPT about an effective overburden stress of 100 kPa. That is, if $\bar{\sigma}_o$ equals 100 kPa, then $\bar{N}$ and N are equal.

Experimental studies by Hardin (1965) suggest that the dissipative potential of sands should be inversely proportional to the initial effective overburden stress. Thus the dissipation function Γ can be written

$$\Gamma(\bar{\sigma}_o,\bar{N}) = \gamma(\bar{N})\sqrt{s/\bar{\sigma}_o} \qquad (6)$$

where s is a characteristic value of stress and $\gamma = \gamma(\bar{N})$ is a dimensionless function of the corrected SPT value to be specified below.

Finally, following Nemat-Nasser and Shokooh (1979), we assume the pore pressure increase at the site, denoted Δu, depends solely on the dissipated energy density, $\Delta\varepsilon$. The exact form of the functional relationship between Δu and $\Delta\varepsilon$ is not known, although we expect Δu to approach $\bar{\sigma}_o$ smoothly as $\Delta\varepsilon$ increases. For Δu smaller than $\bar{\sigma}_o$, we can use the following simple thermodynamic argument to relate Δu and $\Delta\varepsilon$. First suppose all deformations occur at constant volume. Then if all the dissipated energy $\Delta\varepsilon$ is stored in the pore fluid, the pore water temperature will be altered by an amount $\Delta\theta$,

$$\Delta\theta = \Delta\varepsilon/\rho_w c_v \qquad (7)$$

where ρ_w is the pore water density and c_v the pore water constant volume specific heat. The pore pressure increase will be

$$\Delta u = K\alpha\,\Delta\theta \qquad (8)$$

where K and α are the bulk modulus and coefficient of thermal expansion of the pore fluid. Combining equations (7) and (8) gives

$$\Delta u = b\,\Delta\varepsilon \qquad (9)$$

where

$$b = K\alpha/\rho_w c_v \qquad (10)$$

The dimensionless parameter b can be treated as a constant for the relatively moderate changes in temperature and pressure expected. Taking the following typical values for water,

$$K = 2.1 \times 10^6 \text{ kPa}, \quad \alpha = 2 \times 10^{-4}\ {}^\circ C^{-1}$$
$$\rho_w = 10^3 \text{ kg/m}^3, \quad c_v = 4.2 \times 10^3 \text{ J/kg/}^\circ C$$

We find that b equals 0.10.

Combining equations (3), (4), (6), and (9), we now have

$$\Delta u = ab\sqrt{s/\bar{\sigma}_o}\,\gamma(\bar{N})10^{1.5M}/2\pi r^2 \qquad (11)$$

This expression, relating pore pressure increase to earthquake magnitude, epicentral distance, initial overburden stress, and corrected SPT value, is the main result of this article. For a given earthquake (specifying M and r) and given site conditions (specifying $\bar{\sigma}_o$ and $\bar{N}$), equation (10) gives the expected dynamic pore pressure increase at the site. If the expected value of Δu exceeds the initial effective overburden stress, then complete liquefaction is predicted. Values for the constants a and b have been given. Any convenient value for s may be used; we take s = 100 kPa in line with the SPT correction of Peck, Hanson, and Thornburn (1974) given above. It remains, however, to specify the dissipation function $\gamma(\bar{N})$ before equation (11) may actually be used.

ENERGY DISSIPATION AND SPT

In order to establish the form of the dissipation function γ, we employ a statistical analysis of case histories where liquefaction is known to have occurred, or where soils known to be subject to liquefaction have not liquefied in a particular earthquake. Similar analyses have been made by Christian and Swiger (1975) and Yegian and Whitman (1978), but without the basic assumption concerning pore pressure increase and dissipated energy used here. We begin by rearranging equation (11) to have

$$\gamma(\bar{N}) = 2\pi r^2\,\Delta u\sqrt{\bar{\sigma}_o/s}\,10^{-1.5M}/ab \qquad (12)$$

We then define a new function, $\hat{\gamma}$, obtained by replacing Δu in equation (12) by $\bar{\sigma}_o$,

$$\hat{\gamma} = 2\pi r^2\sqrt{\bar{\sigma}_o^{\,3}/s}\,10^{-1.5M}/ab \qquad (13)$$

and we note that if $\Delta u > \bar{\sigma}_o$, then $\gamma > \hat{\gamma}$, while $\Delta u < \bar{\sigma}_o$ implies $\gamma < \hat{\gamma}$. This suggests that we calculate $\hat{\gamma}$ for all case histories where sufficient data exists and plot the resulting values against the corrected SPT value $\bar{N}$ for the sites in question. If liquefaction did occur, the plotted point $(\hat{\gamma}, \bar{N})$ should lie below the actual value of $\gamma(\bar{N})$, while if the site did not liquefy, $(\hat{\gamma},\bar{N})$ should lie above $\gamma(\bar{N})$.

This procedure has been carried out for the 59 case histories listed in Table I, and the resulting graph of $(\hat{\gamma},\bar{N})$ points is shown in Figure 1. In Figure 1, cases where liquefaction was observed are denoted by open circles while cases where liquefaction did not occur are denoted by closed triangles. Although some scatter or intermingling of the liquefied and non-liquefied cases exist, a relatively clear distinction between the two data classes can be seen.

There are a number of sources for error in the data of Figure 1. It should be noted that much of the information in Table I is based on older earthquakes for which epicentral locations and magnitudes are poorly known. Also, the assumption of level ground free from external loads is not satisfied for all case histories, and in many cases SPT values were obtained after the event (sometimes many years after) and would possibly be altered from pre-earthquake values. In some cases, non-isotropic energy radiation, material attenuation, and site effects may have significantly altered the arriving energy content at the site. Finally, in many cases, values for soil density must be assumed in order to calculate initial overburden stresses, and water table elevations may be based on observations made after the earthquake. Considering this variety of error sources, the degree of separation of data shown in Figure 1 is surprisingly good. Two of the cases are bothersome, however. These are events 11 and 17, the San Francisco 1957 earthquake in which liquefaction was observed at Lake Merced, and the San Fernando earthquake in which liquefaction occurred at the site of the Jensen Filtration Plant. These two cases correspond to the two open circles near the top of Figure 1. In the case of the San Fernando earthquake, it is clear that a major portion of the radiated energy was focused into a narrow sector containing the Jensen Plant site (Berrill, 1975). Also both the Jensen Plant and Lake Merced sites were not level ground, and both sites were located at small epicentral distances where anelastic material attenuation effects may have a greater impact on high frequency radiated energy.

A line which best partitions the two classes of data in Figure 1 can now be used to represent the dissipation function $\gamma(\bar{N})$. Although there are different methods for

TABLE I : Liquefaction Case Histories

Event	Site	M	$\bar{\sigma}_o$(kPa)	r(km)	$\bar{N}$	Liq. (?)
1	Ogaki	8.4	135	32	15.3	Yes
1	Ginan West	8.4	99	32	10.1	Yes
1	Unuma	8.4	85	32	20.1	Yes
1	Ogase Pond	8.4	76	32	17.5	Yes
1	Saya	8.4	74	55	15.4	Yes
1	Biwajima	8.4	45	51	20.3	Yes
2	Tone River	7.5	62	79	10.5	No
2	Gyoda	7.5	37	65	10.7	No
2	Kasu	7.5	54	58	12.1	No
2	Kasukabe	7.5	39	37	4.0	Yes
2	Ara River	7.5	47	13	7.5	Yes
3	South of Market	8.3	48	48	8.7	Yes
3	Mission Creek	8.3	69	48	5.6	Yes
3	Salinas	8.3	43	184	10.3	Yes
4	Saya	6.9	74	51	15.4	No
4	Biwajima	6.9	45	57	20.3	No
5	Tone River	7.9	62	114	10.5	No
5	Gyoda	7.9	37	102	10.7	No
5	Kasu	7.9	54	105	12.1	No
5	Kasukabe	7.9	39	96	4.0	Yes
5	Ara River	7.9	47	77	7.5	Yes
5	Ukita	7.9	42	72	6.5	Yes
5	Edogawa	7.9	47	75	15.1	Yes
6	Sheffield Dam	6.3	106	11	2.9	Yes
7	Tone River	7.0	62	20	10.5	Yes
7	Gyoda	7.0	37	19	10.7	Yes
7	Kasu	7.0	54	34	12.1	No
7	Kasukabe	7.0	39	51	4.0	Yes
7	Ara River	7.0	47	65	7.5	No
8	Brawley	7.0	77	8	9.8	Yes
8	All American Canal	7.0	117	8	3.8	Yes
8	Solfatara Canal	7.0	69	8	1.1	Yes
9	Komii	8.3	48	160	5.0	Yes
9	Meiko Street	8.3	28	160	1.4	Yes
10	Miyamae Bridge	7.2	43	12	6.4	Yes
10	Ibatoshuko	7.2	52	10	8.5	Yes
10	Takaya	7.2	91	6.5	18.6	Yes
10	Takaya	7.2	73	6.5	31.0	No
10	Shonenji Temple	7.2	38	6.5	4.0	Yes
10	Agricultural Union	7.2	64	6.5	5.8	Yes
11	Lake Merced	5.5	47	6.5	8.8	Yes
12	Puerto Montt	8.4	70	112	6.7	Yes
12	Puerto Montt	8.4	70	112	9.0	Yes
12	Puerto Montt	8.4	85	112	19.0	No
13	Niigata	7.5	64	51	6.9	Yes
13	Niigata	7.5	64	51	13.8	No
13	Niigata	7.5	99	51	6.0	No
14	Snow River	8.3	58	96	5.9	Yes
14	Snow River	8.3	76	96	5.5	Yes
14	Scott Glacier	8.3	58	88	11.8	Yes
14	Valdez	8.3	60	56	15.2	Yes
15	Hachinohe	7.8	41	65	18.2	No
15	Hachinohe	7.8	41	65	7.8	Yes
15	Hachinohe	7.8	40	65	19.6	No
15	Hokodate	7.8	26	160	5.8	Yes
16	Ebino	6.3	35	7.8	9.5	Yes
17	Jensen Plant	6.4	340	7	11.9	Yes
18	Ishinomaki	7.4	38	82	5.3	Yes
18	Ishinomaki	7.4	38	82	19.8	No.

Notes: Event 1 = Mino Owari, 1891, ref. Kishida (1969) Ishihara (1974)
Event 2 = Tokyo, 1894, ref. Kuribayashi, et al. (1977).
Event 3 = San Francisco, 1906, ref. Youd and Hoose (1976).
Event 4 = Gono, 1909, ref. Ishihara (1974), Kuribayshi, el al. (1975)
Event 5 = Kanto, 1923, ref. Kuribayashi, et al. (1977), Ishihara (1974).
Event 6 = Sanata Barbara, 1925, ref. Seed and Idriss (1970)
Event 7 = Nishi —Saitama, 1931, ref. Kuribayashi, et.al. (1977)
Event 8 = El Centro, 1940, ref. Seed and Idriss (1970)
Event 9 = Tohnanki, 1944, ref. Kishida (1969)
Event 10 = Fukui, 1948, ref. Kishida (1969), Ishihara (1974)
Event 11 = San Francisco, 1957, ref. Seed and Idriss (1970)
Event 12 = Chile, 1960, ref. Seed and Idriss (1970)
Event 13 = Niigata, 1964, ref. Seed and Idriss (1970)
Event 14 = Alaska, 1964, ref. Seed and Idriss (1970)
Event 15 = Tokachioki, 1968, ref. Ohsaki (1970), Kishida (1970)
Event 16 = Ebino, 1968, ref. Yaymonouchi, et al. (1970)
Event 17 = San Fernando, 1971, ref. Dixon and Burke (1973)
Event 18 = Miyagikenoki, 1978, ref. Ishihara, et al.(1980).

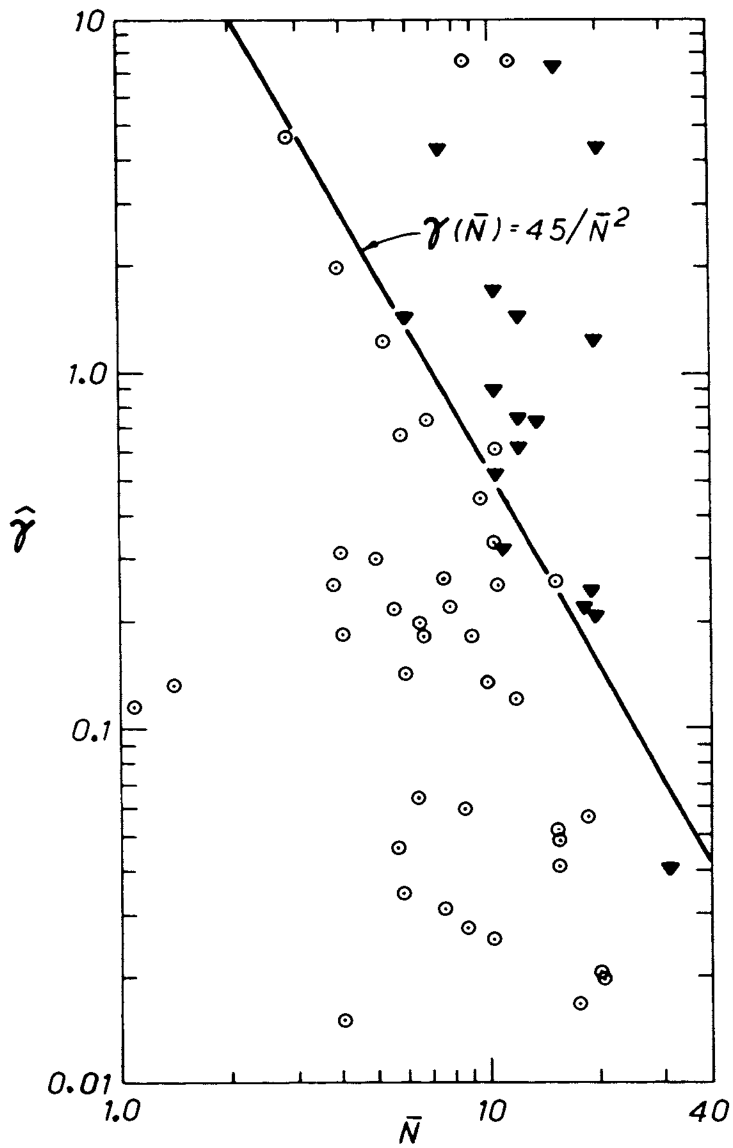

Figure 1. Liquefaction Case Histories.

constructing this partition, a simple statistical method called discriminant analysis (Anderson, 1958) may be easily employed here. The analysis was carried out for all data points in Table I, with the exception of the Lake Merced and Jensen Plant cases which we omit for reasons detailed above. The resulting expression for the dimensionless function γ is

$$\gamma(\bar{N}) = 45/\bar{N}^2 \tag{14}$$

This expression used in equation (11) in conjunction with values for a, b, and s given above, completely specifies the expected dynamic pore pressure increase for given site parameters $\bar{\sigma}_o$ and $\bar{N}$ and given earthquake magnitude and epicentral distance.

DISCUSSION AND CONCLUSIONS

The main result of this work is equation (11), illustrating how dynamic pore pressure build-up may be related to commonly determined parameters which characterize both the site soil conditions and the earthquake which may or may not induce liquefaction. The relationship is based on several simplified assumptions, but its basic form, relating earthquake magnitude and epicentral distance as well as site conditions is both plausible and well suited to assessment of seismic liquefaction risk. It is possible to refine our result in several ways. Anelastic material attenuation may be explicitly considered in obtaining the arriving energy content of seismic waves. The simple, linear Δu-$\Delta \varepsilon$ relationship may be replaced by an experimentally derived formula. And, of course, the definition of the dissipation function $\gamma(\bar{N})$ may be improved as more liquefaction case history data comes to light. Nevertheless, the analysis presented here appears to contain the basic elements necessary for any complete definition of liquefaction potential.

REFERENCES

Anderson, T.W. (1958), "An Introduction to Multivariate Statistical Analysis", John Wiley, New York.

Berrill, J.B. (1975), "A Study of High Frequency Strong Ground Motion From the San Fernando Earthquake", Ph.D. Thesis, California Institute of Technology.

Christian, J.T. and W.F. Swiger (1975), "Statistics of Liquefaction and SPT Results", J. Geotech. Eng. Div. ASCE, (101) GT11, 1135-1150.

Dixon, S.J. and J.W. Burke (1973), "Liquefaction Case History", J. Soil Mech. Found. Div. ASCE, (99) SM11, 921-938.

Gutenberg, B. and C.F. Richter (1956), "Magnitude and Energy of Earthquakes", An. Geofis, (9), 1-15.

Hardin, B.O. (1965), "The Nature of Damping in Sands", J. Soil Mech. Found Div. ASCE, (91)SM1, 63-97.

Ishihara, K. (1974), "Liquefaction of Subsurface Soils During Earthquakes", Technocrat, (7)5, 81-98.

Ishihara, K., Y. Kawase and M. Nakajima (1980), "Liquefaction Characteristics of Sand Deposits at an Oil Tank Site During the 1978 Miyagikenoki Earthquake", Soils and Foundations, (20)2, 97-111.

Kishida, H. (1969), "Characteristics of Liquefied Sands During Mino Owari, Tohnankai, and Fukui Earthquakes", Soils and Foundations, (9)1, 75-92.

Kishida, H. (1970), "Characteristics of Liquefaction of Level Sandy Ground During the Tokachioki Earthquake", Soils and Foundations, (10)2, 103-111.

Kuribayashi, E. and F. Tatsuoka (1975), "Brief Review of Liquefaction During Earthquakes in Japan", Soils and Foundations, (15)4, 81-92.

Kuribayashi, E., T. Iwasaki and F. Tatsuoka (1977), "A History of Soil Liquefaction in Japan", 6th World Conf. Earthquake Eng., New Delhi, 2448-2454.

Nemat-Nasser, S. and A. Shokooh (1979), "A Unified Approach to Densification and Liquefaction of Cohesionless Sand in Cyclic Shearing", Canadian Geotech. J., (16), 659-678.

Ohsaki, Y. (1970), "Effects of Sand Compaction on Liquefaction During the Tokachioki Earthquake", Soils and Foundations, (10)2, 112-128.

Peck, R.B., W.E. Hanson and T.H. Thornburn (1974), "Foundation Engineering", John Wiley, New York.

Seed, H.B. and I.M. Idriss (1970), "A Simplified Procedure for Evaluating Soil Liquefaction Potential", Rep. No. EERC 70-9, Univ. of California, Berkeley.

Yamonouchi, T., S. Taneda and T. Kimura (1970), "Damage Features in the 1968 Ebino Earthquakes from the Viewpoint of Soil Engineering", Soils and Foundations, (10)2, 129-144.

Yegian, M.K. and R.V. Whitman (1978), "Risk Analysis for Ground Failure by Liquefaction", J. Geotech. Eng. Div. ASCE, (104)GT7, 921-938.

Youd, T.L. and S.N. Hoose (1976), "Liquefaction During 1906 San Francisco Earthquake", J. Geotech. Eng. Div. ASCE, (102)GT5, 425-440.